



1 **On the validity of Richards' equation under dynamic flow**  
2 **conditions**

3 **Efstathios Diamantopoulos<sup>1\*</sup>, Sascha Christian Iden<sup>2</sup>**

4 **<sup>1</sup> University of Bayreuth, Chair of Soil Physics**

5 **<sup>2</sup> Technische Universität Braunschweig, Institute of Geoecology, Division of Soil Science**

6 **\* Corresponding author information:** Universität Bayreuth, Fakultät Biologie, Chemie,  
7 Geowissenschaften, 95440 Bayreuth, Germany, Email: Efstathios.Diamantopoulos@uni-  
8 bayreuth.de

9

10 **Abstract**

11 Richards' equation is currently applied to simulate water flow in soils over a wide range of  
12 spatial scales, from the centimeter to the kilometer scale. A key assumption of Richards'  
13 equation is that water content and matric potential are at an equilibrium which is described  
14 by the water retention curve. However, numerous observations have called this  
15 assumption into question, particularly under conditions of fast water flow. In this mini-  
16 review, we present six experiments in which the equilibrium assumption is violated and  
17 which therefore cannot be adequately described by Richards' equation: multistep outflow  
18 / inflow, continuous outflow / inflow, multistep flux, capillary rise, evaporation and,  
19 transpiration. These experiments span a wide range of experimental conditions, from fast  
20 to very slow water flow and apply both pressure head and flux boundary conditions.  
21 Although it is in most cases unknown which exact physical processes are responsible for  
22 these effects, a simple flow model, which extends the Richards equation by a partial  
23 decoupling of pressure head and water content under dynamic flow conditions, can



24 describe the observed relaxation of water content or pressure head well. Notably, this  
25 represents the first demonstration of a non-equilibrium model for all six types of non-  
26 equilibrium observations. We discuss implications, theoretical limitations, and future  
27 perspectives on researching dynamic nonequilibrium in variably-saturated flow in soils, as  
28 well as potential improvements of modeling concepts necessary to describe non-  
29 equilibrium during variably-saturated flow at different scales and under different boundary  
30 conditions.

31



## 32 **1 Introduction**

33 Predicting variably saturated water fluxes, soil water content and water potential in soils  
34 is considered crucial in the environmental sciences, such as hydrology, ecology, and  
35 agricultural science, as the soil's complex biogeochemistry, solute transport, and heat flow  
36 are all influenced by water fluxes and water content. Different theories have been  
37 proposed to model water flow in soils, but until today the Richards equation (RE), which  
38 is grounded in the local mass balance of soil water and the Buckingham-Darcy law for  
39 unsaturated flow, remains undoubtedly the most popular (Nimmo, 2020). The Richards  
40 equation is based on continuum theory and requires averaging of pore scale variables to  
41 macroscopic state variables such as water content and water potential (Bear, 1972). For  
42 the solution of RE, the knowledge of the soil hydraulic properties (SHPs) is required. These  
43 are the water retention curve,  $\theta(h)$ , relating volumetric water content  $\theta$  [ $\text{m}^3 \text{m}^{-3}$ ] to matric  
44 head  $h$  [m], and the hydraulic conductivity curve  $K(h)$  [ $\text{m s}^{-1}$ ]. Although RE has been  
45 applied and is currently applied from the cm (Weller et al., 2011) scale up to kilometer  
46 (Ashby and Falgout, 1996; Kuffour et al., 2020) scale, there is still a lack of understanding  
47 on the relationship between SHPs determined in the laboratory and estimated from field  
48 measurements. Due to structural heterogeneities below the scale of the numerical grid,  
49 the hydraulic equilibrium assumption between  $h$  and  $\theta$  in RE can be violated (Vogel, 2019).  
50 For this reason, the simulation of processes like infiltration and drainage in field soils and  
51 large field lysimeters often do not yield results which are in close enough agreement with  
52 measurements (Vogel, 2019), in particular when soil hydraulic properties measured in the  
53 laboratory are used as material functions, or the effective SHPs obtained from field data  
54 are compared against the ones determined in controlled experiments in the laboratory.



55 One of the reasons for the systematic discrepancy between SHPs (Hannes et al., 2016),  
56 estimated under field and lab conditions is the phenomenon of capillary hysteresis  
57 (Poulovassilis and Childs, 1971; Pham et al., 2005). It refers to the non-uniqueness of the  
58  $\theta(h)$  and its dependence upon the history of soil wetting and drying and has three causes  
59 on the pore scale, (i) the ink bottle effect caused by irregular pore shape (Haines, 1930),  
60 (ii) contact angle hysteresis (Bachmann et al. 2009; Diamantopoulos et al., 2013) and (iii)  
61 shrinkage/swelling effects (Hillel et al., 2007; Pham et al., 2005). Although hysteresis is  
62 recognized as an important process in variably-saturated flow, it is very rarely considered  
63 for larger scale simulation (field and larger), because it requires long and complicated  
64 experiments to adequately parametrize the numerous wetting and drying curves.  
65 Furthermore, given the complexity of real soils (heterogeneity, soil structure variability,  
66 etc.), it is questionable whether incorporating hysteresis leads to decisive improvements  
67 in water flow simulations (Vogel and Roth, 2003).

68 Studying capillary hysteresis and conducting laboratory experiments in general can be  
69 challenging due to the co-occurrence of an additional phenomenon that is difficult to  
70 disentangle from hysteresis (Diamantopoulos et al., 2015; Hannes et al., 2016). Central  
71 assumption to RE, among many others (Diamantopoulos and Durner, 2012), is that water  
72 content and matric potential are tightly coupled through  $\theta(h)$  (or any wetting/drying  
73 scanning curve), independently of whether water does flow or not. This is called the local  
74 equilibrium assumption. The water retention curve is a soil property that reflects the  
75 effective pore-size distribution of the soil and intrinsically accounts for various effects,  
76 water properties, and processes which influence the spatial distribution of water and air in  
77 soils. These encompass (i) surface tension, (ii) the presence of fluid-fluid interfaces, (iii)  
78 wettability of solid surfaces, (iv) the particle size distribution, and (v) micro and macro  
79 heterogeneities. Similarly, the unsaturated hydraulic conductivity function  $K(h)$  or  $K(\theta)$  is



80 influenced by water content, the spatial distribution of air-water interfaces, specific surface  
81 area, roughness of solids, pore tortuosity, and the shape and degree of interconnection of  
82 the water-conducting pores. When using equilibrium  $\theta(h)$  in RE, we assume that all of  
83 these influencing factors have the same effect, regardless of whether water is moving or  
84 not. For  $K(h)$  or  $K(\theta)$ , it is usually assumed that hydraulic conductivity is the same for both  
85 transient and steady-state water flow. Summing up, it is generally assumed that both soil  
86 hydraulic properties are invariant with respect to flow dynamics and therefore identical for  
87 static, steady-state, and transient flow.

88 Starting from the 1960s, many scientists have tested this assumption for various  
89 experimental conditions. Results of those studies show that  $\theta(h)$ , and  $K(h)$  in a lesser  
90 degree, are different between transient and equilibrium conditions (Topp et al., 1967;  
91 Hassanizadeh et al., 1990; Hassanizadeh et al., 2002). This phenomenon is loosely called  
92 “dynamic effects” or “non-equilibrium water flow”. In the following, we will use the acronym  
93 DNE. DNE has been observed in numerous laboratory experiments designed to validate  
94 RE or estimate SHPs: constant flux irrigation wetting/drying experiments (Stonestrom and  
95 Aksin, 1994; Weller et al., 2011; DiCarlo, 2005; 2007), pressure head drainage and  
96 imbibition experiments (Topp et al., 1967; Schultze et al., 1999; O’Carroll, et al.,  
97 2005;2010), and many others (Hassanizadeh et al., 2002; Diamantopoulos and Durner,  
98 2012; Yan et al., 2022). In the field, preferential water flow can be considered as a larger  
99 scale manifestation of DNE (Jarvis, 2007; Ross and Smettem, 2000) which occurs during  
100 infiltration or more generally, during wetting conditions. The occurrence of DNE during  
101 drying is less well researched and it is currently not known if DNE is relevant for drying  
102 conditions. Many different pore-scale processes have also been identified in the literature  
103 as being responsible for DNE. Very briefly, immiscible two-phase interface configuration  
104 (Barenblatt, 1991; Sakaki et al., 2010) dynamic contact angle (Hofmann, 1974; Friedman,



105 1999), air entry effects (Diamantopoulos and Durner, 2012), air (Smiles et al., 1971;  
106 Camps-Roach et al., 2010 ), and water entrapment (Poulovassilis, 1974; Wildenschild et  
107 al., 2001) and/or blockage (Weller et al., 2011), time-dependent water repellency  
108 /hydrophobicity (Reszkowska et al., 2014), fluid properties (Das et al., 2007; Goel and  
109 O'Carroll, 2011) and micro (Mirzaei and Das, 2007) and macroscale heterogeneities  
110 (Manthey et al., 2005). It is important to note, that even if there is hydraulic equilibrium at  
111 the pore scale, spatial averaging may result in DNE at the REV scale (Hassanizadeh et  
112 al., 2002). There is currently no methodology for identifying the dominant cause of DNE  
113 for a specific experiment. Moreover, Wildenschild et al., (2001) suggested that more than  
114 one process can cause DNE for a specific experiment. Summing up, it is difficult to  
115 distinguish which specific processes and causes are responsible for appearances of DNE.

116 Different models to describe DNE have been proposed in the past years. Some of those  
117 are empirical (Barenblatt, 1971; Ross and Smettem, 2000; Diamantopoulos et al., 2012),  
118 while others are based on thermodynamic considerations (Hassanizadeh et al., 2002). For  
119 all models, data-model comparison studies exist, showing that the models are capable of  
120 describing DNE observations (DiCarlo, 2005; O'Carroll et al., 2010; Camps-Roach et al.,  
121 2010). However, model applications are often limited to a single boundary-condition type  
122 and a single porous medium. Although there are some similarities between the different  
123 models, it is currently unclear if those models can describe all or only a subsample of DNE  
124 observations. Moreover, even for the models based on thermodynamic principles, non-  
125 equilibrium parameters can be only estimated through inverse modelling using measured  
126 data with sufficient information content. One special case is provided by the models of  
127 Barenblatt (1971) and Hassanizadeh and Gray (1990) which assume that the faster the  
128 water saturation changes, the more pronounced the DNE becomes.



129 In this contribution, we present experimental results for six different laboratory  
130 observations, and show that RE, with the inherent assumption of hydraulic equilibrium  
131 between  $h$  and  $\theta$ , cannot describe the observed relaxation between water content and the  
132 matric potential. Notably, we also show that this is not only the case for fast water flow  
133 conditions, for which the existence of DNE is currently acknowledged, but that DNE occurs  
134 under slow experiments, too. Despite the different pore scale processes responsible for  
135 the mismatch between RE and the data, we illustrate that a parsimonious effective model  
136 that decouples  $h$  from  $\theta$  under dynamics conditions and includes RE as core component,  
137 can qualitatively describe all experimental data. To the best of our knowledge, this ability  
138 has not been demonstrated by any of the published non-equilibrium models. We conclude  
139 this article with a brief discussion on the relevance of DNE at the field scale, along with  
140 the theoretical limitations and prospects for future research.

## 141 **2 Materials and Methods**

### 142 **2.1 Theory**

#### 143 **2.1.1 Richards equation**

144 Water flow in unsaturated porous media is described by the RE (Richards, 1931), which  
145 in one dimension and without any sink/source terms has the form:

$$\frac{\partial \theta}{\partial t} = \frac{\partial}{\partial z} \left( K(h) \left( \frac{\partial h}{\partial z} + 1 \right) \right) \quad (1)$$

146 where  $\theta$  [ $L^3 L^{-3}$ ] is the volumetric water content,  $t$  [T] is time,  $z$  [L] is the vertical spatial  
147 coordinate (positive upwards),  $h$  [L] is the pressure head, and  $K(h)$  [ $L T^{-1}$ ] is the hydraulic  
148 conductivity function. The numerical solution of Eq. (1) requires the definition of  $\theta(h)$  and



149  $K(h)$ . For all the simulations in this article, the van Genuchten-Mualem model (van  
150 Genuchten, 1980) is used to parametrize the soil hydraulic properties:

$$S(h) = (1 + |\alpha h|^n)^{-m} \quad (2)$$

$$\theta(h) = \begin{cases} \theta_r + (\theta_s - \theta_r)S(h) & h < 0 \\ \theta_s & h \geq 0 \end{cases} \quad (3)$$

$$K(S) = K_s S^l \left[ 1 - (1 - S^{1/m})^m \right]^2 \quad (4)$$

151 where  $S$  [-] is the effective saturation,  $\theta_s$  [ $L^3 L^{-3}$ ] and  $\theta_r$  [ $L^3 L^{-3}$ ] are the saturated and  
152 residual water contents, respectively,  $\alpha$  [ $L^{-1}$ ],  $n > 1$  [-],  $m = 1 - 1/n$  [-], and  $l$  [-] are  
153 shape parameters.

#### 154 **2.1.2 Dual Domain Dynamic Non-Equilibrium model (DUAL-NE)**

155 The DualNE model of Diamantopoulos et al. (2012;2015) assumes that the soil water can  
156 be divided into two distinct fractions or domains. For the first fraction, instantaneous  
157 equilibration between water content and local pressure head is assumed and the soil water  
158 retention curve defines the equilibrium relationship between the two state variables. The  
159 dynamics of unsaturated water flow in this domain are described by RE (Eq. 5). In the  
160 second fraction, some time is required for the equilibration between the water content and  
161 pressure head. This time dependence of the equilibration is described by the non-  
162 equilibrium model of Ross and Smettem (2000). The DualNE model predicts that if the  
163 system has sufficient time to equilibrate, both domains will reach the same equilibrium  
164 state, described by the water retention curve. Assuming that equilibration of the pressure  
165 head between the two domains is relatively fast, the equation of Diamantopoulos et al  
166 (2012) is:



$$(1 - f_{ne}) \frac{\partial \theta_{eq}}{\partial t} + f_{ne} \frac{\partial \theta_{ne}}{\partial t} = \frac{\partial}{\partial z} \left( K(\theta) \left( \frac{\partial h}{\partial z} + 1 \right) \right) \quad (5)$$

167 where  $\theta_{eq}$  [ $L^3L^{-3}$ ] and  $\theta_{neq}$  [ $L^3L^{-3}$ ] are the equilibrium and non-equilibrium volumetric  
168 water contents, respectively, and  $f_{ne}$  [-] is a partitioning parameter having a value between  
169 0 and 1 In the limit of  $f_{ne} = 0$ , Eq. (7) is identical to RE (Eq. 1) and for  $f_{ne} = 1$ , Eq. (5) is  
170 identical to the Ross and Smettem<sup>Error! Bookmark not defined.</sup> approach. For the non-equilibrium  
171 domain, we assume that  $\frac{\partial \theta_{ne}}{\partial t} \cong \frac{\theta_{eq}^* - \theta_{ne}}{\tau}$ , where  $\theta_{eq}^*$  is the equilibrium water content, given  
172 by the equilibrium retention curve and  $\tau$  [T] describes how fast equilibrium is reached  
173 (Ross and Smettem, 2000). As parameter  $\tau$  approaches 0, Eq. 5 converges to RE (Eq. 1).  
174 The model of Diamantopoulos et al. (2012) requires two more parameters than RE,  
175 namely  $f_{ne}$  and  $\tau$ . As previously stated, DualNE is a phenomenological model and the  
176 parameter  $f_{ne}$  and  $\tau$ , can be only estimated through model calibration, contrary to the non-  
177 equilibrium parameter  $\tau_h$  in the model of Hassanisadeh and Gray (1990), which, at least  
178 theoretically, can be estimated from other physical properties (Stauffer, 1978). Both  
179 models, have been implemented in Hydrus 1D (Simunek et al., 1998).

## 180 **2.2 Experimental setups**

181 We tested RE and Dual-NE model against experimental observations from the literature.  
182 The data sets represent six different types of experiments with different boundary  
183 conditions. Table 1 shows the name and type of each experiment, the boundary  
184 conditions, and a reference to the published data. A short description of the experiments  
185 is presented in the results section.

## 186 **3 Evidence of dynamic non-equilibrium und simulations with DUAL-NE model**

### 187 Multistep Outflow/Inflow (MSO/MSI) experiments



188 MSO/MSI experiments are routinely used for the estimation of SHPs in the lab. A soil  
189 column is equipped with one or two tensiometers (Fig 1). At the bottom of the soil column,  
190 a pressure head is applied in an increasing (or decreasing) stepwise manner. The  
191 experiment is simulated with the RE and the SHP of the studied soil are determined by  
192 inverse modeling using a parametric representation of the SHP (Hopmanns et al., 2002).  
193 Nonparametric nonlinear regression has also been applied successfully in the context of  
194 MSO experiments (Bitterlich et al., 2004; Iden and Durner, 2007). After a sudden change  
195 in pressure head at the lower boundary, the pressure head in the soil reaches its  
196 equilibrium (hydrostatic) value quickly whereas the outflow across the bottom shows two  
197 stages (Fig 1a&b). After the pressure change at the bottom boundary, a fraction of water  
198 leaves the soil sample quickly while the pressure head changes (first stage). Afterwards,  
199 while the pressure head in the soil is already constant indicating an apparent hydraulic  
200 equilibrium, a relatively slow drainage of water takes place (second stage, Fig 1a). Similar  
201 dynamics are observed during wetting conditions (Fig 1b) when the pressure head at the  
202 bottom boundary is increased. The dynamics during the second stage cannot be captured  
203 by RE, as it assumes instantaneous local equilibrium between water content and pressure  
204 head. In contrast, the Dual-NE model, as depicted in Fig. 1, accurately represents the  
205 pressure head and cumulative outflow data. Furthermore, it is able to describe an outflow  
206 of water even when the pressure head distribution in the soil column is already in apparent  
207 hydrostatic equilibrium.

#### 208 Continuous outflow/inflow experiments

209 A laboratory experiment similar to MSO/MSI uses a smooth, quasi-continuous change of  
210 the pressure head at the lower boundary. This avoids unnatural, abrupt changes in  
211 pressure head and is therefore closer to real field conditions. In the example shown in



212 Fig. 2, a soil column is continuously drained from 10.2 cm to -60 cm in 192 h and in 3 h,  
213 respectively (Fig 2a). Tensiometers and TDR sensors are installed at the same depth to  
214 measure pressure head and volumetric water content. By pairing the measured data, an  
215 experimental (in-situ) soil water retention curve is obtained. It is obvious that the in-situ  
216 retention curves obtained for the slow and for the fast drainage process differ markedly  
217 (Fig 2c). Based on the  $\theta(h)$  function fitted to the measured outflow and pressure head  
218 data obtained from the slow drainage experiment, both experiments were simulated with  
219 RE. While RE describes the slow (192h) experiment (Fig. 2b) and the slow in situ retention  
220 curve (triangles in Fig 2c), it fails to describe the in-situ retention curve determined under  
221 fast flow conditions (Fig 2c, circles), because there is no difference between fast and slow  
222 drainage for the RE. The Dual-NE model can describe both experiments, with the same  
223 (equilibrium) SHPs and non-equilibrium parameters. This shows that for some part of the  
224 soil water, time is needed to reach equilibrium.

#### 225 Multistep Flux experiment (MSFd/MSFi)

226 In MSF experiments, a water flux is applied across the top of soil column. This flux is either  
227 decreased (MSFd for “drainage”) or increased (MSFi for “imbibition”) in a stepwise  
228 manner. A tensiometer measures the pressure head near the top of the column and the  
229 same pressure head is applied at the bottom of the soil column (Fig 3). By this  
230 experimental design, the column is forced to reach a unit gradient in hydraulic head, in  
231 which case the flux density equals the hydraulic conductivity of the soil  $K(h)$ . An  
232 independent second tensiometer measures the pressure head at the center height of the  
233 soil column. Results show that after a reduction in the applied upper flux (MSFd), the  
234 pressure head drops initially as expected. However, shortly thereafter, it increases  
235 although the water content remains macroscopically constant under the realized steady-



236 state flow conditions. Conversely, a matric potential undershoot is observed for the  
237 imbibition experiment (Fig 3b). While the pressure head dynamics in both cases cannot  
238 be described by RE (Fig 3a: drainage, Fig 3b: imbibition), the Dual-NE model is able to  
239 describe both the overshoot and undershoot occurring under steady-state flow conditions.

#### 240 Capillary rise experiments

241 DNE has also been observed in capillary rise experiments using a constant pressure head  
242 boundary condition at the bottom (Fig 4). In these experiments (Reszkowska, et al., 2014),  
243 soil water flow dynamics are very slow and occur against gravity. A soil column is filled  
244 with dry soil, and it is brought in contact with water at the bottom. The soil column is  
245 equipped with a TDR sensor at a specific height above the water level, and between two  
246 tensiometers (Fig 4a). Tensiometer measurements show that the pressure heads reach  
247 equilibrium with the water table fast (hydrostatic conditions), but water content still  
248 increased for more than 2000 h (Fig 4a). Obviously, the decoupling of water content and  
249 pressure head cannot be described by RE. Once matric potential is at hydrostatic  
250 equilibrium, the RE predicts zero water flow. When the natural soil is mixed with artificially  
251 hydrophobized particles, the effect is more pronounced (Reszkowska et al., 2014) (Fig  
252 4b). Dual-NE can describe the fast equilibration of the matric potential recorded by the two  
253 tensiometer and the slow increase of the water content for both experiments.

#### 254 Transpiration experiments

255 For investigating DNE for the case of slow drying experiments, a simple transpiration  
256 experiment is conducted (Fig 5a). A plant is grown in a soil column and the top of the soil  
257 is covered to minimize evaporation. The column is instrumented with 2 tensiometers,  
258 installed in two different depths. During transpiration, the pressure heads in both depths  
259 have similar values reflecting root water uptake of similar intensity (Fig 5b). Once the



260 transpiration flux is stopped, both tensiometers show an increase in pressure head, even  
261 when the total water content of the soil column does not change (Fig 5b, green line).  
262 Similar effects occur if transpiration is reduced, and not fully stopped (not shown). Due to  
263 the absence of a water sink, the pressure heads converge to different values reflecting a  
264 hydrostatic distribution. The RE with a root water uptake term which is constant in space  
265 cannot describe the increase of pressure head at both depths. Once transpiration stops,  
266 vertical redistribution of water leads to a decrease at the lower position and an increase  
267 at the upper position, but not to an increase in both depths. On the contrary, the Dual-NE  
268 model describes the relaxation of the matric potentials qualitatively, similar to what was  
269 observed in the case of the MSF experiments.

#### 270 Evaporation experiments

271 Another observation of DNE during slow water dynamics can be made in soil evaporation  
272 experiments. A nearly water-saturated soil column is equipped with 2 tensiometers, and  
273 the column is open to the atmosphere at the top. The entire setup is placed on a balance  
274 to monitor water loss and to determine the evaporation rate and the column-averaged  
275 water content (Fig 6). For relatively wet soil profiles (almost linear distribution of matric  
276 potential with depth), a relaxation of all the tensiometer data is observed when the  
277 evaporation flux is stopped. While vertical redistribution of soil water towards hydrostatic  
278 equilibrium would lead to an increase of pressure head at one height and a decrease in  
279 another, the simultaneous increase of pressure head at both heights cannot be described  
280 by RE (Fig 6). During the interruption of evaporation, the soil temperature increases from  
281 15 to 20 °C, following the stop of the latent heat flux and the thermal equilibration with the  
282 surroundings. Although an increase in soil temperature leads to an increase in pressure  
283 head, the magnitude of the temperature effect on pressure head is not large enough to



284 explain the observed increase during the evaporation interruption. As a result of the  
285 observed dynamics, the apparent WRC is “shifting” to the left during the interruption,  
286 indicating that more water is retained by the soil if water flows (Fig 3b). The Dual-NE model  
287 describes the relaxation of the two tensiometer very well. Most importantly, it describes  
288 the dynamics of the evaporation experiment with the equilibrium water retention curve (Fig  
289 3b).

#### 290 **4 Discussion**

291 The phenomenon of DNE describes the decoupling of water content and pressure head  
292 during transient and sometimes even during steady-state flow. The phenomenon  
293 contradicts the local equilibrium assumptions which is the basis for simulating variably-  
294 saturated flow with the RE. As a result, the RE often fails to describe flow experiments in  
295 which pressure head and water content are monitored.

296 One result of DNE is the flow-rate dependence of soil hydraulic properties. Examples for  
297 the dependency of the water retention curve on flow conditions have been presented in  
298 chapter 3. Even in well-sorted and packed soil materials, the identified retention curve  
299  $\theta(h)$  depends on whether it is determined under static, slow or fast dynamic flow  
300 conditions. In the case of dynamic drainage, more water is withheld by the soil at the same  
301 pressure head compared to the static case. The opposite is observed for imbibition  
302 experiments. This has not only been observed for fast water flow, as it was previously  
303 believed, but also for relatively slow water dynamics occurring during evaporation,  
304 transpiration, and capillary rise.

305 It is noteworthy that the physical mechanisms accountable for DNE in the six distinct  
306 experiments outlined in chapter 3 differ from one another. For example, water entrapment  
307 may explain DNE in MSO and MSF type of experiments but not in the capillary rise



308 experiments. To explain the occurrence of DNE in slow experiments such as evaporation,  
309 transpiration, and capillary rise, it seems reasonable to consider the influence of sub-REV  
310 scale heterogeneities in surface energy and wettability. This is because the faster  
311 dynamics, required for phase entrapment, or dynamic contact angle are not relevant for  
312 these slow processes. As pointed out by other researchers (Wildenschild et al., 2001), it  
313 is possible that DNE may arise from more than one physical process, which complicates  
314 the design of experiments to disentangle the exact underlying mechanisms. At a  
315 macroscopic level, all six observations presented here can be explained by the following  
316 mechanism: certain accessible pore paths are responsible for initiating flow after a change  
317 in boundary conditions. However, behind the wetting or drying front, a second stage of  
318 (horizontal) equilibration occurs involving a relatively small amount of water between pores  
319 of varying sizes within the REV. This secondary stage of equilibration is not instantaneous  
320 and is responsible for the time-varying, and thus non-unique, behavior of the water  
321 retention curve  $\theta(h)$  at the REV scale.

322 Although multiple factors can simultaneously drive DNE in dynamic flow experiments,  
323 which makes it difficult to pinpoint the dominant cause(s), we demonstrated that the DUAL-  
324 NE model, which partially decouples water content from pressure head, can describe all  
325 observations at the macroscopic scale. We neither suggest to replace the RE by the more  
326 general Dual-NE model in all cases, nor argue that research aimed at identifying the  
327 precise physical processes responsible for DNE should be abandoned. Rather, and given  
328 the complexity of DNE, it is crucial for the soil hydrologic community to acknowledge these  
329 effects in laboratory experiments and to consider potential biases when interpreting data.  
330 The Dual-NE model can be a valuable tool for quantitatively comparing DNE across  
331 various experiments and different materials or evaluating standard laboratory  
332 experiments. For example, in the evaporation experiment (Fig 6), the model can be used



333 to estimate the equilibrium  $\theta(h)$  instead of the dynamic one. Of course, this would require  
334 simple modifications to the experimental procedure, for instance the inclusion of flow  
335 interruptions, an established technique in column breakthrough experiments, at least in  
336 the majority of cases in which the non-equilibrium parameters are unknown. Moreover,  
337 targeted experiments are necessary to improve our understanding of DNE and to identify  
338 potential biases resulting from it. This is very important for studying the combined effect  
339 of DNE and hysteresis, since it is expected that there will be a difference between dynamic  
340 and equilibrium hysteretic scanning curves. Moreover, it is crucial to investigate how  
341 different intensities of boundary condition changes (or saturation changes), different  
342 materials (i.e., packed, structured), and different spatial scales (cm, dm, m) affect the non-  
343 equilibrium parameters of the Dual-NE model. Can the Dual-NE model describe different  
344 experiments conducted at the same system (type, imbibition, drying, etc.) with the same  
345 set of SHPs for one material, and the same non-equilibrium parameters? And, if this is not  
346 the case, how do these parameters differ for the different boundary conditions, and for  
347 different water contents or pressure heads. Recent advances in information science  
348 suggest that combining the flexibility of a model such as Dual-NE with statistical learning  
349 methods may eventually lead to the development of more accurate prediction tools.

350 Many scientists hold the view that DNE occurs only in (rapid) laboratory experiments and  
351 are questioning its relevance for field conditions. However, at the plot scale, preferential  
352 water flow can also be regarded as expression of DNE. The Ross and Smettem **Error!**  
353 **Bookmark not defined.** model, which is a special case of the Dual-NE model if  $f_{ne}=1$ ,  
354 was originally developed to effectively describe fast, preferential water flow through soils.  
355 For this model, it is essential to use  $K(h)$  rather than the  $K(\theta)$  formulation currently used  
356 in Dual-NE (Eq. 5). This means that a reevaluation of the conductivity function is necessary



357 to extend Dual-NE for describing preferential water flow. While there are some initial ideas  
358 on this topic (Vogel et al., 2022), further testing of all the experiments mentioned above is  
359 necessary to demonstrate the generalizability of any new approach. It is also worth noting  
360 that even when the RE is applied at the hectometer or kilometer scale, its parametrization  
361 typically relies indirectly on laboratory experiments, because pedotransfer functions (Van  
362 Looy et al., 2017; Weber et al., 2024) are based on lab data. This means that DNE  
363 occurring in lab experiments may indirectly affect large scale simulations. In contrast to  
364 DNE during infiltration, the relevance of DNE at the plot scale under drainage conditions  
365 remains to be explored. For field drainage, flux densities similar to those encountered in  
366 the reported evaporation (0.12 mm/h) and transpiration experiments (1.9 mm/h) are  
367 expected. This calls again for multiscale experiments on DNE, that include drying and  
368 wetting conditions.

## 369 **5 Conclusion**

370 In this mini-review, we presented evidence of dynamic non-equilibrium (DNE) effects in  
371 six types of laboratory experiments covering a wide range of boundary conditions and flow  
372 rates. The results demonstrate that the decoupling of water content and pressure head is  
373 not restricted to fast water flow conditions, as previously believed, but also occurs under  
374 slow dynamics such as evaporation, transpiration, and capillary rise. The RE, with its  
375 inherent local equilibrium assumption, systematically fails to describe these observations.  
376 A simple extension of the RE, the Dual-NE model, which decouples water content from  
377 pressure head in a subdomain of the soil, was able to qualitatively reproduce all six  
378 experiments. This suggests that a single and relatively simple modeling approach might  
379 be capable of describing DNE in a consistent manner. While we do not advocate replacing  
380 the Richards equation in all applications, these findings highlight the need for the soil



381 hydrology community to acknowledge DNE effects when designing and interpreting  
382 laboratory experiments. Future work should focus on multi-scale experiments under both  
383 wetting and drying conditions, the interplay between DNE and hysteresis, work towards a  
384 unified DNE framework that can additionally simulate preferential water flow, and the  
385 potential use of statistical learning methods to improve the predictive capability of non-  
386 equilibrium models.

#### 387 **Code Availability**

388 The code for this work will be made available upon acceptance of the manuscript.

#### 389 **Data Availability**

390 The data for this work will be made available upon acceptance of the manuscript.

391

#### 392 **Acknowledgments**

393

394 The authors acknowledge using ChatGPT (<https://chatgpt.com/>) to review language  
395 usage and enhance readability. After using this tool, the authors reviewed and edited the  
396 manuscript, and take full responsibility for its content. This work was carried out in the  
397 framework of the project „DynSoilWater“ funded by the German Research Foundation  
398 (DFG) under grants DI2146/3-1 and ID 75/2-1.

399



400 **References**

401

402 Ashby, S. F. and Falgout, R. D.: A Parallel Multigrid Preconditioned Conjugate Gradient  
403 Algorithm for Groundwater Flow Simulations, Nucl. Sci. Eng., 124, 145–159, 1996.

404 Bachmann, J., Woche, S.K., Goebel, M.O., Kirkham, M.B., Horton, R., 2003. Extended  
405 methodology for determining wetting properties of porous media. Water Resour. Res.  
406 39, 1353–1365. Barari, A., Omidvar, M., Ghotbi, A.R., and D.D. Ganji, (2009),  
407 Numerical analysis of Richards problem for water penetration in unsaturated soils,  
408 Hydrology and Earth System Sciences, <https://doi.org/10.5194/hessd-6-6359-2009>

409 Barenblatt, G.I. 1971. Filtration of two nonmixing fluids in a homogeneous porous  
410 medium. Fluid Dyn. 6:857–864.

411 Barenblatt, G.I., 1971. Filtration of two mixing fluids in a homogeneous porous medium,  
412 Fluid. Dyn. 6:857-864

413 Bear, J. 1972. Dynamics of fluids in porous media. American Elsevier, New York.

414 Bitterlich, S., Durner, W., Iden, S.C. and Knabner, P. (2004), Inverse Estimation of the  
415 Unsaturated Soil Hydraulic Properties from Column Outflow Experiments Using Free-  
416 Form Parameterizations. Vadose Zone Journal, 3: 971-981.  
417 <https://doi.org/10.2136/vzj2004.0971>

418 Camps-Roach, G., D.M. O'Carroll, T.A. Newson, T. Sakaki, and T.H. Illangasekare. 2010.  
419 Experimental investigation of dynamic effects in capillary pressure: Grain size  
420 dependency and upscaling. Water Resour. Res. 46:W08544.  
421 doi:10.1029/2009WR008881



- 422 Das, B.D., Gaudie, R., Mirzaei, M., 2007. Dynamic effects for two-phase flow in porous  
423 media: fluid property effects. *AIChE J.* 53 (10), 2505–2520.
- 424 Diamantopoulos, E., and W. Durner, 2012. Dynamic nonequilibrium of water flow in  
425 porous media: A review, *Vadose Zone J.*, doi:10.2136/vzj2011.0197
- 426 Diamantopoulos, E., and W. Durner, 2012. Dynamic nonequilibrium of water flow in  
427 porous media: A review, *Vadose Zone J.*, doi:10.2136/vzj2011.0197
- 428 Diamantopoulos, E., Durner, W., Reszkowska, A. and Bachmann, J., 2013. Effect of soil  
429 water repellency on soil hydraulic properties estimated under dynamic conditions,  
430 *Journal of Hydrology*, 10.1016/j.jhydrol.2013.01.020
- 431 Diamantopoulos, E., I.C. Iden, and W. Durner. 2012. Inverse modeling of dynamic non-  
432 equilibrium in water flow with an effective approach. *Water Resour. Res.* 48:W03503.  
433 doi:10.1029/2011WR010717
- 434 Diamantopoulos, E., W. Durner, S. Iden, U. Weller, and H.-J. Vogel. 2015. Modeling  
435 dynamic non-equilibrium water flow observations under various boundary conditions.  
436 *J. Hydrol.* 529:1851–1858. doi:10.1016/j.jhydrol.2015.07.032
- 437 DiCarlo, D.A. 2005. Modeling observed saturation overshoot with continuum additions to  
438 standard unsaturated theory. *Adv. Water Resour.* 28:1021–1027.  
439 doi:10.1016/j.advwatres.2004.12.003
- 440 DiCarlo, D.A. 2007. Capillary pressure overshoot as a function of imbibition flux and initial  
441 water content. *Water Resour. Res.* 43:W08402. doi:10.1029/2006WR005550
- 442 Friedman, S.P. 1999. Dynamic contact angle explanation of flow rate-dependent  
443 saturation–pressure relationships during transient liquid flow in unsaturated porous



444 media. J. Adhes. Sci. Technol. 13: 1495– 1518.

445 <https://doi.org/10.1163/156856199X00613>

446 Goel, G., and D.M. O'Carroll. 2011. Experimental investigate on of nonequilibrium

447 capillarity effects: Fluid viscosity effects. Water Resour. Res. 47:W09507.

448 doi:10.1029/2010WR009861

449 Haines, W. B. (1930), Studies in the physical properties of soil. V. The hysteresis effect

450 in capillary properties, and the modes of moisture distribution associated therewith, J.

451 Agric. Sci., 20, 97– 116, doi:10.1017/S002185960008864X.

452 Hannes, M., Wolschlaeger, U., Woehling, T., and H.-Vogel, 2016. Revisiting hydraulic

453 hysteresis based on long-term monitoring of hydraulic states in lysimeters, Water

454 Resour. Res., <https://doi.org/10.1002/2015WR018319>

455 Hassanizadeh, S.M., and W.G. Gray. 1990. Mechanics and thermodynamics of

456 multiphase flow in porous media including interphase boundaries. Adv. Water Resour.

457 13:169–186. doi:10.1016/0309-1708(90)90040-B

458 Hassanizadeh, S.M., M.A. Celia, and H.K. Dahle. 2002. Dynamic effects in capillary

459 pressure–saturation relationships and its impact on unsaturated flow. Vadose Zone J.

460 1:38–57

461 Hillel, 1998. Environmental Soil Physics Academic Press, San Diego (1998), 7771 pp

462 Hillel, D., Pham HQ, Fredlund DG, Barbour SL. 2005. A study of hysteresis model for

463 soil-water characteristic curves. Canadian Geotechnical Journal 42: 1548–1568.

464 Hoffman, R.L. 1975. Study of advancing interface: 1. Interface shape in liquid–gas

465 systems. J. Colloid Interface Sci. 50: 228– 241. <https://doi.org/10.1016/0021->

466 9797(75)90225-8



- 467 Hopmans, J.W., Simunek, J., Romano, N., Durner, W., 2002. Simultaneous determination  
468 of water transmission and retention properties – inverse methods. In: Dane, J.H., Topp,  
469 G.C. (Eds.), *Methods of Soil Analysis, Part 4. SSSA Book Ser. 5.* SSSA, Madison, WI,  
470 pp. 963–1008.
- 471 Iden S.C., and W. Durner (2007): Free-Form estimation of the unsaturated soil hydraulic  
472 properties by inverse modelling using global optimization, *Water Resources Research*,  
473 doi:10.1029/2006WR005845
- 474 Jarvis, N.J., 2007. A review of non-equilibrium water flow and solute transport in soil  
475 macropores: Principles, controlling factors and consequences for water quality. *Eur.*  
476 *J. Soil Sci.*, 58:523-546. Doil:10.1111/j.1365-2389.2007.00915.x
- 477 Kuffour B.N.O., Engdahl, N.B., Woodward, C.S., Condon, L.E., Kollet, S., R. M. Maxwell,  
478 2020. Simulating coupled surface–subsurface flows with ParFlow v3.5.0: capabilities,  
479 applications, and ongoing development of an open-source, massively parallel,  
480 integrated hydrologic model, *Geosci. Model Dev.*, 13, 1373–1397, 2020,  
481 <https://doi.org/10.5194/gmd-13-1373-2020>
- 482 Manthey, S., S.M. Hassanizadeh, and R. Helmig. 2005. Macro-scale dynamic effects in  
483 homogeneous and heterogeneous porous media. *Transp. Porous Media* 58:121–145.  
484 doi:10.1007/s11242-004-5472-6
- 485 Mirzaei, M., and B.S. Das. 2007. Dynamic effects in capillary pressure saturation  
486 relationships for two-phase flow in 3D porous media: Implication of micro-  
487 heterogeneities. *Chem. Eng. Sci.* 62:1927–1947. doi:10.1016/j.ces.2006.12.039
- 488 Nimmo, J.R., (2020), The processes of preferential flow in the unsaturated zone, *Soil*  
489 *Science Society of America Journal [Invited Review]*, doi:10.1002/saj2.20143



- 490 O'Carroll, D.M., K.G. Mumford, L.M. Abriola, and J.I. Gerhard. 2010. Influence of  
491 wettability variations on dynamic effects in capillary pressure. *Water Resour. Res.*  
492 46:W08505. doi:10.1029/2009WR008712
- 493 O'Carroll, D.M., T.J. Phelan, and L.M. Abriola. 2005. Exploring dynamic effects in  
494 capillary pressure in multistep outflow experiments. *Water Resour. Res.* 41:W11419.  
495 doi:10.1029/2005WR004010
- 496 Pham HQ, Fredlund DG, Barbour SL. 2005. A study of hysteresis model for soil-water  
497 characteristic curves. *Canadian Geotechnical Journal* 42: 1548–1568.
- 498 Poulouvasilis, A. 1974. The uniqueness of the moisture characteristics. *Soil Sci.* 25:27–  
499 33. doi:10.1111/j.1365-2389.1974.tb01099.x
- 500 Poulouvasilis, A., and E. C. Childs (1971), The hysteresis of pore water: The non-  
501 independence of domains, *Soil Sci.*, 112(5), 301–312
- 502 Reszkowska, A., Bachmann, J., A. Lamparter, Diamantopoulos, E., and W. Durner. 2014.  
503 The effect of temperature-induced soil water repellency on transient capillary  
504 pressure-water content relations during capillary rise. *European Journal of Soil*  
505 *Science*, 2014, 64, 369-376, doi: 10.1111/ejss.12139
- 506 Richards, L.A. 1931. Capillary conduction of liquids through porous media. *Physics*  
507 1:318–333. doi:10.1063/1.1745010
- 508 Ross, P.J., and K.R.J. Smettem. 2000. A simple treatment of physical nonequilibrium  
509 water flow in soils. *Soil Sci. Soc. Am. J.* 64:1926–1930.  
510 doi:10.2136/sssaj2000.6461926x



- 511 Sakaki, T., D. M., O`Carroll and T.H. Illangasekare, 2010. Direct quantification of dynamic  
512 effects in capillary pressure for drainage-wetting cycles. *Vadose Zone Journal*, 9:424-  
513 437, doi:10.2136/vzj2009.0105
- 514 Schultze, B., O. Ippisch, B. Huwe, and W. Durner. 1999. Dynamic nonequilibrium in  
515 unsaturated water flow. In: M.Th. van Genuchten et al., editors, *Proceedings of an*  
516 *International Workshop on Characterization and Measurement of the Hydraulic*  
517 *Properties of Unsaturated Porous Media*, Riverside, CA. 22–24 Oct. 1997. Univ. of  
518 California, Riverside. p. 877–892.
- 519 Simunek, J., M. Sejna, and M. Th. Van Genuchten, 1998. The Hydrus-1D software  
520 package for simulating the one-dimensional movement of water, heat and multiple  
521 solutes in variably-saturated media. Version 2.0, IGWMC-TPS-70, International  
522 Ground Water Modelling Center, Colorado School of Mines, Golden, CO. 202
- 523 Smiles, D.E., G. Vachaud, and M. Vauclin. 1971. A test of the uniqueness of the soil  
524 moisture characteristic during transient, nonhysteretic flow of water in a rigid soil. *Soil*  
525 *Sci. Soc. Am. Proc.* 35:534–539. doi:10.2136/sssaj1971.03615995003500040018x
- 526 Stauffer, F. 1978. Time dependence of the relationships between capillary pressure water  
527 content and conductivity during drainage of porous media. In: *IAHR Symposium on*  
528 *scale Effects in porous media*, Thessaloniki, Grece. 29 Aug-1 Sept 1978. *Int. Assoc*  
529 *Hydro-Environ. Eng. Res.*, Madrid, Spain, p.3.35-3.53.
- 530 Stonestrom, D.A., and K.C. Aksø n. 1994. Nonmonotonic matric pressure histories  
531 during constant flux infiltration into homogeneous profiles. *Water Resour. Res.* 30:81–  
532 91. doi:10.1029/93WR02476



- 533 Topp, G.C., A. Klute, and D.B. Peters. 1967. Comparison of water content– pressure  
534 head data obtained by equilibrium, steady-state, and un- steady-state methods. Soil  
535 Sci. Soc. Am. Proc. 31:312–314. doi:10.2136/ sssaj1967.03615995003100030009x
- 536 van Genuchten, M.Th. 1980. A closed-form equation for predicting the hydraulic  
537 conductivity of unsaturated soils. Soil Sci. Soc. Am. J. 44:892–898.  
538 doi:10.2136/sssaj1980.03615995004400050002x
- 539 Van Looy, K., Bouma, J., Herbst, M., Koestel, J., Minasny, B., Mishra, U., Montzka, C.,  
540 Nemes, A., Pachepsky, Y., Padarian, J., Schaap, M.G., Tóth, B., Verhoef, A.,  
541 Vanderborght, J., van der Ploeg, M.J., Weihermüller, L., Zacharias, S., Zhang, Y.,  
542 Vereecken, H., 2017. Pedotransfer functions in Earth System Science: Challenges  
543 and Perspectives, Review of Geophysics, <https://doi.org/10.1002/2017RG000581>
- 544 Vogel, H.J., 2019. Scale issues in soil hydrology. Vadose Zone j.,  
545 doi:10.2136/vzj2019.01.0001
- 546 Vogel, H.J., and K., Roth, 2003. Moving through scales of flow and transport in soil, J.  
547 Hydrol., [https://doi.org/10.1016/S0022-1694\(02\)00257-3](https://doi.org/10.1016/S0022-1694(02)00257-3)
- 548 Vogel, H.J., Gerke, H. H., Mietch, R., Zahl, R., Wöhling, T., 2022. Soil hydraulic  
549 conductivity in the state of nonequilibrium, Vadose Zone Journal, 2023,e20238
- 550 Weber, KDT et al., 2024, Hydro-pedotransfer functions: a roadmap for future  
551 development, <https://doi.org/10.5194/hess-28-3391-2024>
- 552 Weller, U., O. Ippisch, J.M. Köhne, and H.J. Vogel. 2011. Direct measurement of  
553 unsaturated hydraulic conductivty including nonequilibrium and hyster-esis. Vadose  
554 Zone J. 10:654–661. doi:10.2136/vzj2010.0074



555 Wildenschild, D., J.W. Hopmans, and J. Šimůnek. 2001. Flow rate dependence of soil  
556 hydraulic characteristics. Soil Sci. Soc. Am. J. 65:35–48.  
557 doi:10.2136/sssaj2001.65135x

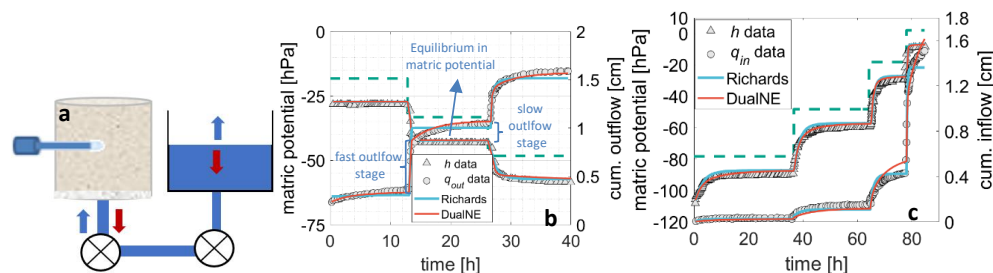
558 Yan, G., Li, Z., Torres, S.A.G., Scheuermann, A., and Li, L., 2022, Transient Two-Phase  
559 flow in Porous media: A literature review and Engineering Application in Geotechnics,  
560 Geotechnics, <http://doi.org/10.3390/geotecvhnichs2010003>

561



562 **Figures and Tables**

563



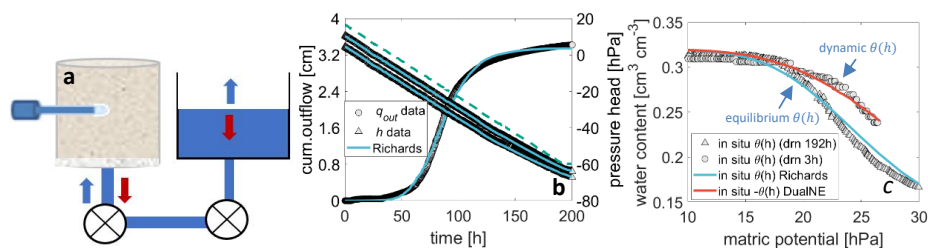
564

565

566 **Figure 1.** Schematic diagram of experimental setup for the multistep outflow and inflow  
 567 experiments (a). The pressure head at the lower boundary is varied in a stepwise manner (green  
 568 dashed line in b, c). During drainage, the pressure head reaches equilibrium quickly, but the  
 569 outflow dynamics show two stages. In the first stage, water outflow is rapid while the pressure  
 570 head changes. This is followed by a slower equilibration under an apparent hydrostatic pressure  
 571 distribution (b). Similarly, a two-stage inflow is observed during imbibition experiments (c).  
 572 Although Richards' equation describes the dynamics and equilibration of the matric potential data,  
 573 it fails to mimic the dynamics of the cumulative outflow (b) or inflow (c). In contrast, both  
 574 experiments can be described by the Dual-NE approach, where the water content is divided into  
 575 two fractions, one which equilibrates quickly with pressure head, and one which lags behind.

576

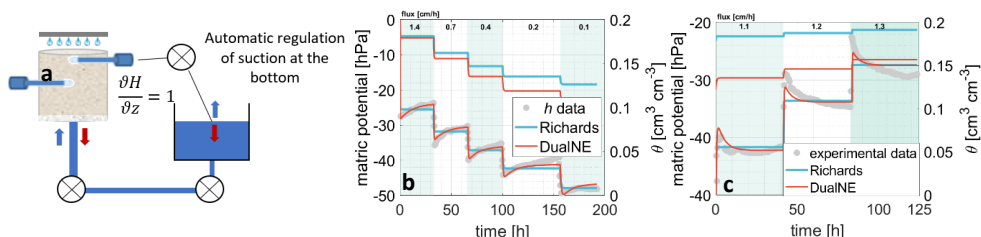
577



578

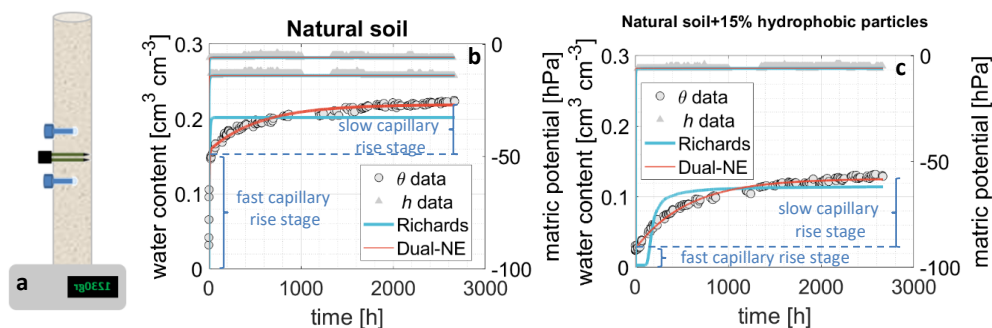
579 **Figure 2.** Schematic diagram of the experimental setup for continuous outflow experiments (a).

580 The pressure head at the lower boundary is changed continuously (green line in b) under slow  
 581 drainage. Richards' equation can adequately describe the pressure head and cumulative outflow  
 582 data for slow drainage (b), as well as the slow in-situ retention curve (c). However, it fails to  
 583 describe the retention curve obtained from the fast experiment (circles in c). For fast flow,  
 584 Richards' equation predicts the same equilibrium curve, regardless of the flow conditions. In  
 585 contrast, the Dual-NE model can describe both experiments using the same set of soil hydraulic  
 586 properties and non-equilibrium parameters.



587

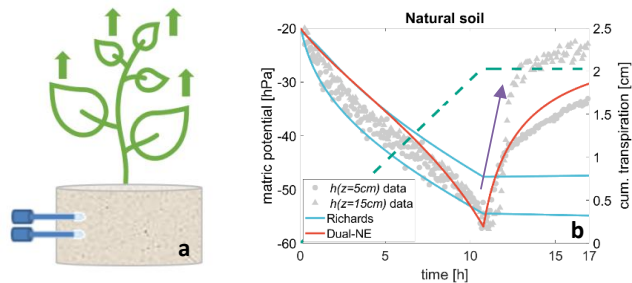
588 **Figure 3.** Schematic diagram of the experimental setup for the multistep flux experiment (a). An  
 589 irrigation flux is either reduced (drainage experiment, b) or increased (wetting experiment, c) at  
 590 the top of the soil column. A tensiometer is used to measure the pressure head near the soil  
 591 surface, and the same pressure is applied at the bottom of the soil column, forcing the system to  
 592 reach unit gradient conditions, as shown in a. For the drainage experiment (MSFd, b), once the  
 593 flux is reduced, the matric potential measured by an independent tensiometer is also reduced as  
 594 expected, but then it slowly rises again. The opposite is observed for the wetting experiment (c).  
 595 This behavior cannot be described by the Richards equation since it predicts constant matric  
 596 potential and water content throughout the column once steady-state conditions are reached. On  
 597 the other hand, the Dual-NE model can describe both overshoot (b) and undershoot (c) in  
 598 pressure head.



599

600 **Figure 4.** Schematic diagram of the experimental setup for capillary rise experiments (a). An  
 601 initially dry soil is brought into contact with water, and the water in the column rises against  
 602 gravity. The soil column is equipped with two tensiometers and one TDR installed between the  
 603 two tensiometers (a). The data show that the two tensiometers equilibrate very quickly with the  
 604 water level. However, the water content measured by the TDR keeps increasing, and the soil  
 605 continues to absorb water for more than 2500 hours or more than 105 days (b). This effect is  
 606 more pronounced for a mixture of a natural soil with 15% hydrophobic particles, where only one  
 607 tensiometer is used (c). Richards' equation describes the fast equilibration of the matric potential  
 608 data but fails to describe the two-stage equilibration of the water content. This is because, once  
 609 equilibrium in matric potential is reached, Richards' equation predicts equilibrium in water content  
 610 as well (blue line b, c). In contrast, the Dual-NE model predicts both the matric potential data and  
 611 the two-stage water content data well (b, c).

612



613

614 **Figure 5.** Schematic diagram of the experimental setup for the transpiration experiment (a).

615 Initially, a soil column with high water content and two installed tensiometers is allowed to

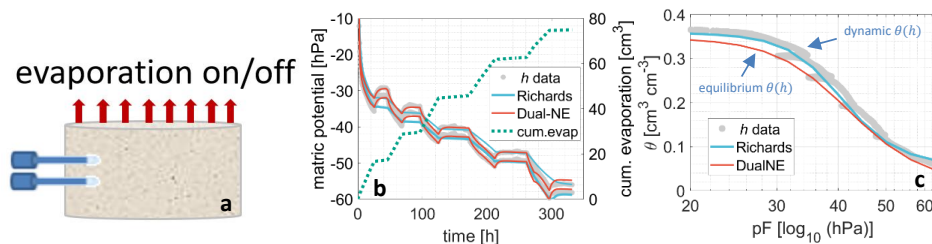
616 transpire. When the transpiration flux is stopped, both tensiometers show a relaxation towards

617 higher pressure head (purple arrow in b). This cannot be adequately described by Richards'

618 equation (blue lines in b). In contrast, the Dual-NE model can qualitatively describe the relaxation

619 in matric potential (red line in b).

620



621

622 **Figure 6.** Schematic diagram of the experimental setup for the evaporation experiment (a). An  
623 initially wet soil column, equipped with two tensiometers, evaporates across the top boundary.  
624 The evaporation is stopped repeatedly by covering the soil surface. The recorded data from all  
625 the tensiometers show a relaxation towards higher pressure heads, which cannot be described by  
626 the Richards equation (b). By plotting the data as a water retention curve, it becomes evident that  
627 the retention curve measured under dynamic conditions is shifted to the left during the flow  
628 interruptions, towards the equilibrium retention curve (c). The Dual-NE model can effectively  
629 describe the dynamics of the matric potential and most importantly, it can do so with the  
630 equilibrium water retention curve.

631

632

633



634 **Table 1.** Overview of the experimental setups for all the experiments, including the type of  
635 boundary condition used. More detailed information on the experimental design can be obtained  
636 from the cited references.  
637

Name	Boundary condition	Type	Reference
multistep outflow/inflow	pressure head (stepwise)	wetting/drying	Diamantopoulos et al (2013)
continuous outflow	pressure head (smooth)	drying	Schultze et al (1999)
multistep Flux	flux	wetting/drying	Weller et al (2011)
capillary rise	pressure head	wetting	Reszkowska et al (2014)
transpiration	flux (sink)	drying	Unpublished data (Diamantopoulos, University of Bayreuth)
evaporation	flux	drying	Diamantopoulos and Durner (2012)

638